VOLUME 39 NUMBER 6
ACCOUNTS of CHEMICAL RESEARCH®
JUNE 2006

Generating Function Methods in Single-Molecule Spectroscopy

FRANK L. H. BROWN
Department of Chemistry and Biochemistry, University of California, Santa Barbara, California 93106-9510

Received July 25, 2005

ABSTRACT
Certain single-molecule measurements record a time series of individual physical events. Examples of such events include the emission of single photons or discrete fluctuations of molecular state (as in fluorescence blinking or spectral diffusion). The generating function formalism is a natural framework for studying these measurements both theoretically and numerically. Kinetic, stochastic, and quantum models for chromophore dynamics may all be extended to generating function calculations, enabling direct comparison to experiment with only slight extensions to familiar theoretical/computational tools.

I. Introduction

The introduction of single-molecule experimental techniques just over a decade ago[1,2] has revolutionized the study of condensed-phase systems in chemistry, physics, and biology. While certain single-molecule studies focus on systems where dynamics are directly observable via microscopy,[3−6] frequently it is necessary to extract information from spectroscopic signals (see reviews in refs 7−11 and references therein). More often than not, interpretation of single-molecule experiments is a complicated affair.

All molecules but the largest biopolymers are too small to be studied with light microscopes and most molecular motions are far too fast to be studied with video-rate cameras. This leaves spectroscopy as the primary means of studying single molecules and their dynamics. In single-molecule spectroscopy (SMS) experiments, laser irradiation of single chromophoric molecules induces fluorescence of photons. The fluoresced photons are detected; their arrival times, and possibly frequency information as well, serve as the experimental data. SMS spectroscopy, unlike traditional spectroscopies, is inherently a study of a discrete data stream. Every collected photon results from a single spontaneous emission event, and it is the time history of these emissions registered in experiment. Even in experiments where single-photon resolution is not achieved, experimental data is often condensed into a form where it is possible to assign a set of discrete time points as a representation of the full data set (as in on/off blinking experiments[12]).

SMS experiments are inherently noisy, not only due to imperfections in detection schemes but also due to the inherent physical stochasticity in the spontaneous emission process and the ubiquitous presence of thermal fluctuations over molecular length scales. While SMS has been hailed for its ability to probe these fluctuations directly, it remains difficult to extract physical pictures for molecular dynamics based solely on SMS data streams. Some of this difficulty is likely fundamental (current SMS experiments may not collect sufficient data to allow for direct inversion to molecular dynamics), but even if SMS data were sufficient to differentiate among all viable physical hypotheses, it remains an open question as to the best means to simulate such models to allow for comparison with experiment. Indeed, much effort has been expended on the theory of interpreting/modeling SMS trajectories (see reviews in refs 12 and 13 and references therein).

Generating function (GF) methods are a well-established technique in statistics for dealing with discrete random events in time.[14] In chemical physics texts,[15,16] the GF is often introduced as an elegant and concise means to derive classical results related to Poisson processes, 1-D random walks, and similar toy problems. It is apparently not widely appreciated, however, that these same tech-

Frank Brown was born in Menlo Park, CA, on October 12, 1972. He received a B.A. in Applied Mathematics and a B.S. in Chemistry from UC Berkeley in 1994 and a Ph.D. in Physical Chemistry from MIT in 1998. After holding postdoctoral positions at UC San Diego and the University of Chicago, he joined the Chemistry and Biochemistry faculty at UC Santa Barbara in 2001 where he is currently an Assistant Professor. He is an Alfred P. Sloan Research Fellow and was awarded the Presidential Early Career Award for Scientists and Engineers (PECASE) in 2004. His research deals with a variety of theoretical problems in physical chemistry and biophysics.

10.1021/ar050028l CCC: $33.50
Published on Web 04/26/2006

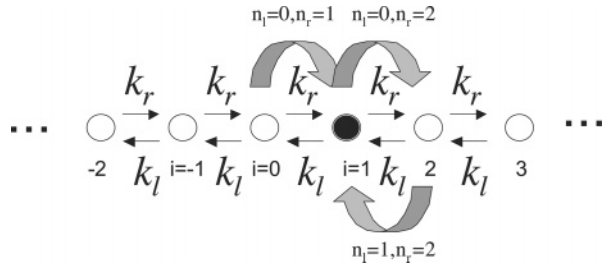

FIGURE 1. A random walk beginning at the origin. Here three discrete jumps have occurred, two to the right followed by one to the left. The current position of the walker is $i = 1$ with $n_l = 1$ and $n_r = 2$.

niques are easily extended to complex physical models appropriate to SMS and that the resulting equations are well suited to numerical analysis as well as traditional analytical work. In many ways, the GF technique is completely natural for the study of SMS trajectories. GFs were introduced to the field of SMS independently by Brown[17] and Gopich and Szabo[18] in the context of kinetic and stochastic models for dynamics. Zheng and Brown[19,20] and Mukamel[21] extended this picture to quantum dynamics for single chromophores, much in the spirit of earlier work by Cook.[22] Multiple studies in SMS have since applied the generating function approach[23−29] to various physical models and situations relevant to SMS.

This Account presents an introduction to the GF method with examples of how this formalism may be applied to the field of SMS. The following section introduces the concept of GFs within the context of a simple random walk model. Section III extends this discussion to a kinetic/stochastic description of single-molecule photon emission statistics. Although quantum mechanics (section IV) complicates the technical details necessary to perform calculations, all important concepts are clearly displayed within this simple kinetic picture. Sections V and VI wrap up with some examples of the GF formalism applied to SMS including quantum mechanical dynamics of the chromophore. The examples chosen in this work assume individual photon emissions to be the observable stochastic events. Blinking experiments turn out to be mathematically identical but are not specifically discussed in the interest of brevity.

II. Generating Functions Introduced

Some elementary properties of GFs are introduced here in the context of a simple random walk model. Consider a one-dimensional random walk in continuous time that begins at the origin (Figure 1). At a given instant in time, the walker is found at a site indexed by an integer i. The walker remains at this site until he randomly decides to hop (either left or right) to an adjacent site. Suppose we track the total number of leftwards and rightwards jumps that have occurred up to time t. Call these numbers n_l and n_r, respectively. (Note that since $n_r - n_l = i$, tracking the number and direction of all jumps provides more information than following i alone.)

If the walker's decision to stay put, jump left, or jump right in a short time interval is completely independent of his prior history, it is possible to formulate the stochastic dynamics of his travels in terms of an infinite master equation.

$$\frac{\mathrm{d}}{\mathrm{d}t}p_{n_l,n_r}(t) = -(k_r + k_l)p_{n_l,n_r}(t) + k_r p_{n_l,n_r-1}(t) + k_l p_{n_l-1,n_r}(t) \quad (1)$$

Here it is assumed that each site is equivalent to all others in the sense that the rate to jump left is always k_l and the rate to jump right is always k_r; $p_{n_l,n_r}(t)$ is the probability that the walker has made exactly n_l left jumps and n_r right jumps prior to time t. Equation 1 implies an infinite set of equations because the number of possible jumps is unlimited.

A convenient way to solve eq 1 is to introduce two "auxiliary"[15] variables, s_l and s_r, and the associated GF

$$G(s_l,s_r,t) \equiv \sum_{n_l,n_r=0}^{\infty} p_{n_l n_r}(t) s_l^{n_l} s_r^{n_r} \quad (2)$$

Multiplication of eq 1 by $s_l^{n_l} s_r^{n_r}$ and summing over all nonnegative integer values for n_l and n_r leads to a single equation for the GF

$$\frac{\partial}{\partial t}G(s_l,s_r,t) = [-k_r - k_l + k_r s_r + k_l s_l]G(s_l,s_r,t) \quad (3)$$

with the solution

$$G(s_l,s_r,t) = \exp[-k_l(1 - s_l)t]\,\exp[-k_r(1 - s_r)t] \quad (4)$$

This equation expresses the fact that the joint probability distribution for left and right jumps reflects two statistically independent Poisson distributions, a conclusion that might have been obvious from the nature of the walk. To see this, expand eq 4 in a Taylor series in s_l and s_r and compare terms to definition 2 to find

$$p_{n_l,n_r}(t) = \mathrm{e}^{-k_l t}\frac{(k_l t)^{n_l}}{n_l!}\,\mathrm{e}^{-k_r t}\frac{(k_r t)^{n_r}}{n_r!} \quad (5)$$

(Alternately, differentiating eq 4 multiple times with respect to s_l, s_r, or both and evaluation at $s_l = s_r = 0$ will yield the same result.) The distribution of the walker's position along the line follows immediately

$$P_i(t) = \sum_{n_l,n_r=0}^{\infty} p_{n_l,n_r}(t)\delta_{n_r-n_l,i} = \mathrm{e}^{-(k_l+k_r)t}\sum_{n_l=0}^{\infty}{}' \frac{(k_l t)^{n_l}}{n_l!}\frac{(k_r t)^{n_l+i}}{(n_l+i)!} \quad (6)$$

where the prime on the sum indicates a restriction to values of n_l such that $(n_l + i)$ is nonnegative. This sum can be shown to approach a Gaussian distribution as time approaches infinity.[15] The mean and variance of this distribution are conveniently calculated using an extremely useful property of $G(s_l,s_r,t)$

$$\frac{\partial^a}{\partial s_l^a}\frac{\partial^b}{\partial s_r^b} G(s_l,s_r,t)|_{s_l=s_r=1} =$$
$$\langle n_l(n_l-1)...(n_l-a+1)n_r(n_r-1)...(n_r-b+1)\rangle(t) \quad (7)$$

which follows immediately by differentiating through the sum of eq 2. We exploit this general result to calculate

$$\langle i\rangle(t) = \langle n_r - n_l\rangle(t) = (k_r - k_l)t \quad (8)$$

$$[\langle i^2\rangle - \langle i\rangle^2](t) = [\langle (n_r - n_l)^2\rangle - \langle i\rangle^2](t) = (k_r + k_l)t \quad (9)$$

and the associated Gaussian approximation to the distribution that becomes increasingly accurate as time progresses

$$P(i,t) \approx \frac{1}{\sqrt{2\pi(k_r+k_l)t}}\exp\left[\frac{-(i-(k_r-k_l)t)^2}{2(k_r+k_l)t}\right] \quad (10)$$

The preceding example was chosen to illustrate the following characteristics of the GF approach relevant to single-molecule spectroscopy:

1. Introduction of the GF reduces an infinite number of coupled equations to a finite number of dynamic equations of motion (one in the above case) at the expense of introducing new continuous auxiliary variables.

2. The conversion from the normal dynamical equations of motion (eom) to equations for the generation function is relatively simple, involving only strategic placement of the auxiliary variables within the ordinary eom.

3. With a solution for the GF in hand it is possible to extract the probabilities associated with the original formulation of the problem and statistical moments for the occurrence of events under investigation. These quantities come from differentiating the GF itself.

4. It is possible to track multiple types of events (forward and backward jumps in the above) within a single GF eom; each type of event is associated with a unique auxiliary variable.

III. Generating Functions for Photon Emission: Kinetic Treatment

The most fundamental event observable to SMS is the emission of individual photons. With only minor modification, the above treatment is easily extended to models for photon counting. In the simplest possible scheme, we imagine a two-state chromophore under laser excitation centered at the transition frequency. We assume that the exciting light is spectrally broader than the intrinsic line width of the chromophore. Under this condition, the excitation from ground to excited state is incoherent, as is the spontaneous emission from excited to ground.[30]

Were we only interested in the behavior of the chromophore itself (to the exclusion of photon-counting information), we would formulate the dynamics in terms of the simple master equation implied by the left panel of Figure 2

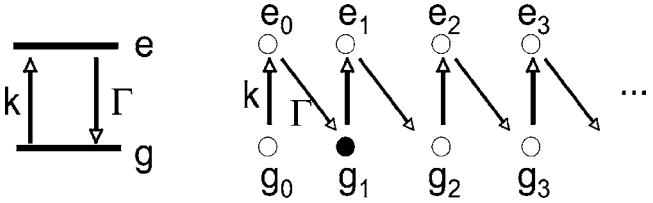

FIGURE 2. Kinetic model for two-level chromophore photon emission under excitation. In the left panel, the instantaneous electronic state is either ground (g) or excited (e) with Markovian (rate process) transitions allowed between the two. Dynamics are governed by the usual master equation approach applied to the two level system. In the right panel, to study the process of photon emission, the state space is expanded to track the total number of photon emissions that have occurred since the field was turned on. Allowable states are g_n and e_n with n any nonnegative integer. In addition to the electronic state, the index n counts the number of previously emitted photons. Spontaneous emission via Γ necessarily advances this index by one. The shaded circle indicates that the system currently resides in the ground electronic state and has previously emitted one photon.

$$\frac{d}{dt}\begin{pmatrix}P_g(t)\\P_e(t)\end{pmatrix} = \begin{pmatrix}-k & \Gamma\\ k & -\Gamma\end{pmatrix}\cdot\begin{pmatrix}P_g(t)\\P_e(t)\end{pmatrix} \quad (11)$$

Here, P_g and P_e are the probabilities to find the chromophore in the ground and excited states, respectively. Tracking photon statistics is impossible with this approach even though the decay from excited to ground state is necessarily accompanied by the emission of a photon.

Photon emission information is included by considering the infinite master equation suggested by the extended kinetic scheme in the right panel of Figure 2

$$\frac{d}{dt}P_{g_n}(t) = -kP_{g_n} + \Gamma P_{e_{n-1}}$$
$$\frac{d}{dt}P_{e_n}(t) = kP_{g_n} - \Gamma P_{e_n} \quad (12)$$

In this formulation, we have refined our definition of a state to include not only the chromophore's electronic configuration, but also the number of prior photon emissions that have occurred. Accordingly, the probabilities P_{g_n} and P_{e_n} reflect the probabilities to find the chromophore in the ground or excited state with a past history of n photon emissions.

In analogy to the preceding section, we define GFs for each of the indexed probabilities

$$G_g(s,t) = \sum_{n=0}^{\infty} P_{g_n}(t)s^n$$
$$G_e(s,t) = \sum_{n=0}^{\infty} P_{e_n}(t)s^n \quad (13)$$

Multiplication of eqs 12 by s^n followed by summing over n leads to equations of motion for the GFs

$$\frac{d}{dt}\begin{pmatrix}G_g(s,t)\\G_e(s,t)\end{pmatrix} = \begin{pmatrix}-k & s\Gamma\\ k & -\Gamma\end{pmatrix}\cdot\begin{pmatrix}G_g(s,t)\\G_e(s,t)\end{pmatrix} \equiv \mathbb{M}(s)\cdot\tilde{G}(s,t) \quad (14)$$

with the solution

$$\tilde{G}(s,t) = \exp \mathbb{M}(s)t\cdot\tilde{G}(s,0) = \exp \mathbb{M}(s)t\cdot\begin{pmatrix}P_g(0)\\P_e(0)\end{pmatrix} \quad (15)$$

Extraction of photon-counting statistics proceeds as in our previous example. The only difference is that now we have two GFs corresponding to the ground- and excited-state manifolds. Experiment, however, is sensitive only to n and not to electronic state. The GF for photon emission events is thus $G(s,t) = G_g(s,t) + G_e(s,t)$, which counts all contributions to the photon statistics irrespective of the instantaneous electronic state. The final expression is analytically tractable since $\mathbb{M}$ is diagonalizable

$$G(s,t) = \frac{e^{-[(\Gamma+k-f(s))t/2]}(\Gamma + k + f(s)) - e^{-[(\Gamma+k+f(s))t/2]}(\Gamma + k - f(s))}{2f(s)}$$

$$f(s) \equiv \sqrt{(\Gamma - k)^2 + 4\Gamma k s} \quad (16)$$

(Note that this particular answer assumes that the system began in the ground state at time $t = 0$. See Figure 3 for the effect of different initial conditions.)

Although this model is very simple, it does contain sufficient physics to explore many of the ideas associated with general photon-counting measurements. Parameters k and Γ represent the only physical parameters of this model, reflecting the rate of field-induced electronic excitation and the rate of spontaneous emission. The average rate of photon emission is calculated in a straightforward, if algebraically tedious, manner as

$$\text{emission rate} \equiv \lim_{t\to\infty}\frac{d}{dt}\langle n\rangle = \lim_{t\to\infty}\frac{d}{dt}\left(\left.\frac{\partial G(s,t)}{\partial s}\right|_{s=1}\right) = \frac{\Gamma k}{(k+\Gamma)} \quad (17)$$

The second moment of photon emission is traditionally reported in terms of Mandel's Q parameter[31]

$$Q \equiv \lim_{t\to\infty}\frac{\langle n^2\rangle - \langle n\rangle^2 - \langle n\rangle}{\langle n\rangle} = \lim_{t\to\infty}\frac{\left(\left.\frac{\partial^2 G(s,t)}{\partial s^2}\right|_{s=1}\right) - \langle n\rangle^2}{\langle n\rangle} = -\frac{2\Gamma k}{(\Gamma + k)^2} \quad (18)$$

The above expressions may also be calculated outside the long time limit, but the answers reflect the initial condition of the system, explicit time dependence as the steady state is approached, and are algebraically much more complicated. Figure 3 graphs the results of such calculations including time dependence.

Physically, the above expressions are readily interpreted. The steady-state ($t \to \infty$) limit for emission rate is expected to be given by the steady-state probability that the chromophore is found in its excited state times the rate of emission from this state. From eq 11, the steady-state limit $P_e(\text{s.s.}) = k/(k + \Gamma)$ is determined. The spontaneous emission rate is Γ, and the rate of photon emission follows immediately. Calculation of Q from physical principles is complicated by the fact that $\langle n^2\rangle(t)$ requires information on two photon correlations by virtue of the relation[15]

$$\langle n^2\rangle(t) = \int_0^t dt_1 \int_0^t dt_2\, P(t_1,t_2) = 2\Gamma^2\int_0^t dt_1 \int_0^{t_1} dt_2\, P_e(\text{s.s.})\hat{P}_e(t_1|t_2) + \Gamma t P_e(\text{s.s.}) \quad (19)$$

In the first equality, $P(t_1,t_2)$ is the probability density that the system emits photons at times t_1 and t_2. This density contains contributions from two distinct photons for $t_1 \neq t_2$ and individual photons when $t_1 = t_2$. The probability density for single-photon emission at a given time is expected to be the product of Γ and the excited-state probability at that time, which leads to the indicated contribution due to single-photon effects within $P(t_1,t_2)$. $\hat{P}_e(t_1|t_2)$ is the conditional probability that the system is found in its excited state at time t_1 when it was in the ground state at t_2, and the two-photon contribution follows when it is recalled that photon emission necessarily dumps the molecule into the ground state. The expression $\hat{P}_e(t_1|t_2) = P_e(\text{s.s.})(1 - \exp(-(k + \Gamma)(t_1 - t_2)))$ may be inferred from eq 11. Inserting this in eq 19 leads to eq 18 in the limit of large t.

The fact that Q saturates to a negative value is the mathematical signature of photon antibunching. Since spontaneous emission necessarily localizes the electron to the ground state, it is impossible for two successive photon emissions to occur immediately after one another. It takes some time for the system to cycle back to the excited state to allow for a second emission event. Only in the limit of $k/\Gamma = 0$ or $\Gamma/k = 0$ will Q vanish. In the case that $k \ll \Gamma$, for example, eq 16 reduces to

$$G(s,t) = e^{-k(1-s)t} \quad (k \ll \Gamma) \quad (20)$$

with the associated Poissonian distribution

$$p_n(t) = \frac{(kt)^n}{n!}e^{-kt} \quad (21)$$

In the opposite limit ($\Gamma \ll k$), we find analogous expressions, but with Γ substituted for k. In either extreme case, the slow rate becomes limiting in the problem, and this rate defines an exponential waiting time distribution between photon emission events, that is, a Poissonian process and $Q = 0$. In more general situations, the distributions associated with eq 16 are algebraically complicated. $Q < 0$ reflects the fact that finite k and Γ lead to a correlation between successive emission events and that the emission times are accordingly less randomly distributed than a pure Poisson process. Interestingly, $Q < 0$ can be taken as an experimental signature that you are in fact observing a single chromophore[32] (in practice, most experiments report the equivalent quantity $\hat{P}_e(t_1|t_2)$).

From a practical standpoint, it is convenient to calculate low-order photon counting moments directly without having to calculate the full GF (especially when analytical solutions are not available). This is accomplished by differentiating eq 14 with respect to s one or more times. The resulting equations for $\partial^m\tilde{G}/\partial s^m$ depend on the lower

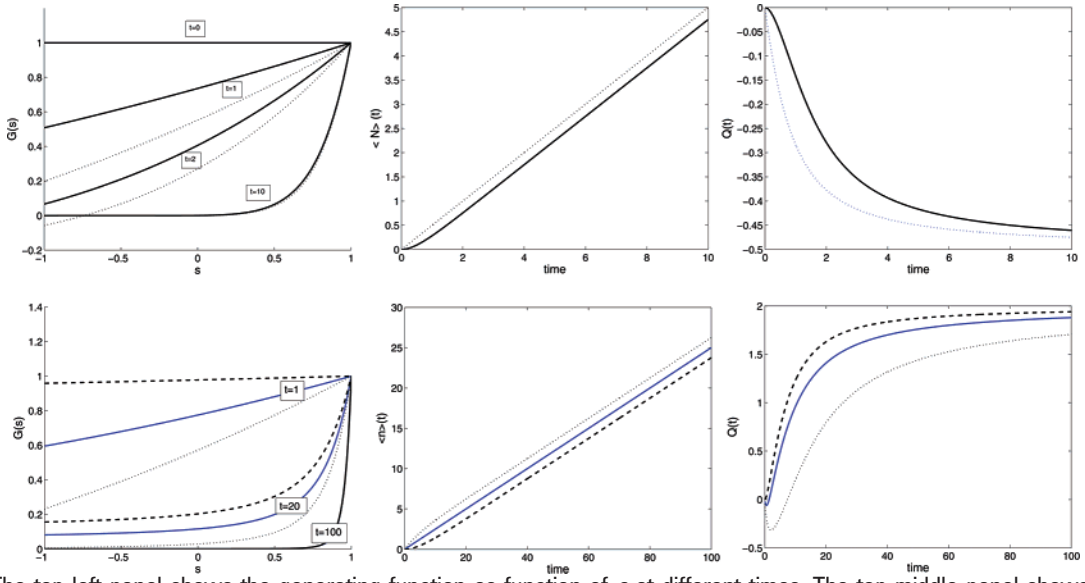

FIGURE 3. The top left panel shows the generating function as function of s at different times. The top middle panel shows the average number of emitted photons, $\langle n\rangle(t)$. The top right panel shows Mandel's Q parameter, $Q(t)$. We have assumed the model of Figure 3 with parameter values $\Gamma = k = 1$ in arbitrary time units. In all upper panels, solid lines correspond to expression 16, which assumes that the system begins in the ground state at $t = 0$. Dotted lines assume a steady-state initial condition, $P_g(0) = P_e(0) = {}^1/_2$. At short times the initial condition makes a difference, but the effect is quickly washed out. The bottom panels show similar calculations to the top ones but considering the case of a chromophore coupled to a stochastic two-level system. We have chosen $\omega_{ab} = \omega_{ba} = 0.1$ and the same chromophore parameters as in the top panels for the "a" state, but $k_b = \Gamma_b = 0$. That is, the a state corresponds to a system that is fluorescing and absorbing, while the b state is totally inactive. The different lines correspond to different initial conditions. All three reflect equilibrium between electronic states. The solid line additionally reflects equilibrium between a and b, the dotted line reflects full occupation of the a state at time 0, and the dashed reflects full occupation of b at $t = 0$.

order derivatives of $\tilde{G}$ in a simple way.[20] Up to second order, for example, we find

$$\begin{pmatrix} \dot{\tilde{G}}(s,t) \\ \dfrac{\partial \dot{\tilde{G}}(s,t)}{\partial s} \\ \dfrac{\partial^2 \dot{\tilde{G}}(s,t)}{\partial s^2} \end{pmatrix} = \begin{pmatrix} \mathbb{M}(s) & 0 & 0 \\ \mathbb{M}'(s) & \mathbb{M}(s) & 0 \\ 0 & 2\mathbb{M}'(s) & \mathbb{M}(s) \end{pmatrix} \cdot \begin{pmatrix} \tilde{G}(s,t) \\ \dfrac{\partial \tilde{G}(s,t)}{\partial s} \\ \dfrac{\partial^2 \tilde{G}(s,t)}{\partial s^2} \end{pmatrix} \quad (22)$$

The prime notation indicates differentiation with respect to s. Higher order derivatives on $\mathbb{M}(s)$ do not appear since these higher derivatives all vanish. The matrix implied by the block form used above is actually 6×6 for the present model but is still easily solved numerically by direct exponentiation. Since s derivatives of $G(s,t)$ evaluated at $s = 1$ correspond directly with photon emission moments by virtue of eq 7, solving the above equations at $s = 1$ yields $\langle n\rangle(t)$ and $Q(t)$ immediately. This method was used in the generation of Figure 3. (If one is only interested in the steady-state values of the various moments, and not their time dependence, an even simpler computational scheme may be formulated.[29])

For this simple example, it is perhaps unclear why one would want to introduce the generating function approach. We have shown simple physical arguments to arrive at the first two moments and could even go further to show that all higher moments only depend on quantities we have already discussed in this case. The true utility of the GF comes into play when we consider more complex models for dynamics. A simple physically motivated extension to the above model is to consider the case that k and Γ may themselves be fluctuating in time due to stochastic modulation by the environment. A particularly simple form of modulation is two-state jump dynamics.[15] In addition to ground and excited electronic states, we imagine an additional discrete degree of freedom that jumps in time between two states a and b. Such a model is standard in the study of low-temperature glasses[33] where the two states represent localized conformational states of the glass, the so-called two-level system (TLS) model. This additional degree of freedom evolves with dynamics specified by the master equation

$$\begin{pmatrix} \dot{P}_a(t) \\ \dot{P}_b(t) \end{pmatrix} = \begin{pmatrix} -\omega_{ab} & \omega_{ba} \\ \omega_{ab} & -\omega_{ba} \end{pmatrix} \cdot \begin{pmatrix} P_a(t) \\ P_b(t) \end{pmatrix} \quad (23)$$

and through the properties of composite Markov processes[15,17,34] leads to the GF equations for this four-state system

$$\frac{\mathrm{d}}{\mathrm{d}t}\begin{pmatrix} G_{g;a}(s,t) \\ G_{e;a}(s,t) \\ G_{g;b}(s,t) \\ G_{e;b}(s,t) \end{pmatrix} = \begin{pmatrix} -k_a - \omega_{ab} & s\Gamma_a & \omega_{ba} & 0 \\ k_a & -\Gamma_a - \omega_{ab} & 0 & \omega_{ba} \\ \omega_{ab} & 0 & -k_b - \omega_{ba} & s\Gamma_b \\ 0 & \omega_{ab} & k_b & -\Gamma_b - \omega_{ba} \end{pmatrix} \cdot \begin{pmatrix} G_{g;a}(s,t) \\ G_{e;a}(s,t) \\ G_{g;b}(s,t) \\ G_{e;b}(s,t) \end{pmatrix} \equiv \mathbb{M}(s) \cdot \tilde{G}(s,t) \quad (24)$$

$k_{a(b)}$ and $\Gamma_{a(b)}$ are the rates for chromophore excitation and emission when the TLS occupies state $a(b)$. The beautiful thing is that the more complicated system of equations here (relative to eq 14) is, as the notation implies, formally equivalent to the simpler dynamics. In particular, calculation of moments still proceeds via eq 22. Once you can write down the usual master equation for system dynamics, it is a simple matter to generalize this expression to $\mathbb{M}(s)$. With $\mathbb{M}(s)$ and $\mathbb{M}'(s)$ in hand, the matrix of eq 14 is constructed from these blocks, multiplied against time and exponentiated to arrive at the moments. *If you know the system's dynamics in terms of a master equation, it is a trivial numerical procedure to extend this master equation to a calculation of photon-counting moments.* In fact, using a high-level programing language like Matlab or Mathematica, it takes about five lines of code to generate photon-counting moments once the master equation is specified! Numerical results are illustrated in Figure 3 for the case of TLS dynamics an order of magnitude slower than the photon emission rates and with extreme coupling to the chromophore such that k_a and Γ_a assume the values introduced previously, but $k_b = \Gamma_b = 0$. The rate of photon emission is halved relative to the earlier model since the system only spends half its time in the emitting state. Q now saturates to a positive value, reflecting photon bunching. Photons are only emitted when the system is in the a state, which leads to long dark intervals in the photon emission trajectory. Saturation to the value 2 reflects this bunching phenomena (which alone would predict $Q \rightarrow {}^5/_2$), but tempered a bit by the intrinsic negative values for Q inherent to the emitting state.

This section has introduced all the relevant ideas necessary for calculation of photon-counting moments for models based around stochastic dynamics. The main points established here include the following items extending those points brought up in section II:

5. Internal states of the chromophore pose no difficulty in formulating a GF description of photon counting. In the case of stochastic models, the master equation is modified by inclusion of the auxiliary variable s to create the GF equations of motion.

6. Placement of the auxiliary variables in the formation of $\mathbb{M}(s)$ is elementary. At every occurrence of $+\Gamma$ in the master equation transition matrix, make the replacement $+\Gamma \rightarrow +s\Gamma$. If there are multiple types of photon emission being followed (as in two-color detection schemes[25]) individual spontaneous emission terms of the form $+\Gamma_\alpha$ are multiplied by the corresponding auxiliary variable s_α. Note that the $-\Gamma$ terms are never multiplied by an auxiliary variable.

7. For models that are not analytically solvable, it is often most convenient to calculate low-order photon-counting moments by numerically solving the exact equations 22 that couple photon moments up to order m with all lower order moments. The numerical calculation corresponds to exponentiation of a $(m+1)\cdot N \times (m+1)\cdot N$ matrix where N is the total number of internal states accessible to the chromophore system (i.e., $N \times N$ is the size of the corresponding transition matrix for the associated master equation). It takes almost no programming effort to perform this calculation once the master equation is known. Of course, if N becomes large, matrix exponentiation will be slow.

8. Markovian stochastic environmental modulation of the chromophore is easily handled through the mathematical techniques established in the context of composite Markovian processes[15] or dynamical disorder.[34] The matrices to be exponentiated become larger, but the underlying theoretical treatment for the GF approach remains unchanged.

IV. Generating Functions for Photon Emission: Quantum Treatment

In the preceding section, a fairly detailed account was provided for the generating function route toward photon statistics in the context of completely stochastic models for dynamics. We shall not formally extend these arguments to the quantum case here (interested readers should consult refs 20 and 21 for the detailed analysis), but rather appeal to simple arguments.

Within the stochastic picture, chromophore dynamics are formulated in terms of a master equation, symbolically written as

$$\dot{\tilde{P}}(t) = \mathbb{M}(s{=}1)\cdot\tilde{P}(t) \tag{25}$$

where $\tilde{P}(t)$ is the vector of state probabilities and $\mathbb{M}(s)$ is equivalent to the transition matrix when $s = 1$. Generalizing to arbitrary s leads immediately to the GF equations of motion so long as the replacement $\tilde{P}(t) \rightarrow \tilde{G}(s,t)$ is made concurrently. Correspondence with quantum mechanical systems proceeds via the density matrix formalism and relies upon the assumption that photon emission events are treated as incoherent rate processes. We introduce a linear superoperator $\mathbb{L}$, which acts upon the density matrix to effect time evolution in the quantum mechanical system,

$$\dot{\rho}(t) = \mathbb{L}\rho(t) \tag{26}$$

It is most convenient to think of $\rho(t)$ as a vector of dimension N^2 containing all populations and coherences for a system with N quantum states and $\mathbb{L}$ as an $N^2 \times N^2$ matrix for the reduced system dynamics. The radiation field will not be considered quantum mechanically (hence "reduced dynamics"). Exciting fields are treated classically, and spontaneous emission is handled by integrating out the field variables to provide elements within $\mathbb{L}$ corresponding to the emission process(es).[30,35] Within the usual approximations, this leads to spontaneous emission occurring as a Markovian rate process that dumps chromophore population from upper to lower electronic state manifolds.

As in the case of stochastic dynamics, we convert eq 26 to a GF picture by appending auxiliary variables s_α to those matrix elements of $\mathbb{L}$ that cause population to appear in lower electronic states as a result of spontaneous emission processes. The index α distinguishes between

the various allowed spontaneous-emission-mediated transitions (i.e., rovibronic structure and multiple electronic states). By following every transition individually, it becomes possible to separately monitor statistics of photons from each transition. In the case of spectrally resolved molecular transitions, this provides a route to emission spectra and higher order moments resolved into colors. Or, all transitions can be assigned the same auxiliary variable to determine photon statistics for broadband detection. From a formal perspective, we arrive at equations identical in structure to the stochastic case (For notational simplicity, the below assumes all photon emissions are counted equivalently and only a single s variable is introduced.)

$$\dot{\tilde{G}}(s,t) = \mathbb{L}(s)\cdot\tilde{G}(s,t)$$

$$G_{ab}(s,t) = \sum_{n=0}^{\infty}\rho_{ab_n}(t)s^n \tag{27}$$

Since the elements of ρ (and hence $\tilde{G}$) represent populations and coherences of the density matrix, they are accordingly indexed by two labels. As always, the subscript n refers to the number of prior photon emissions in our expanded description of dynamics. For the actual extraction of moments, it is important to remember that coherences do not contribute to probabilities, so that

$$1 = \sum_{a=1}^{N}\rho_{aa}(t) = \sum_{a=1}^{N}G_{aa}(1,t)$$

$$\langle n\rangle(t) = \sum_{a=1}^{N}\left.\frac{\partial G_{aa}(s,t)}{\partial s}\right|_{s=1}$$

$$\langle n(n-1)\rangle(t) = \sum_{a=1}^{N}\left.\frac{\partial^2 G_{aa}(s,t)}{\partial s^2}\right|_{s=1} \tag{28}$$

etc.

Only those portions of $\tilde{G}(s,t)$ and its s derivatives corresponding to populations contribute to the moments in the quantum case. With this single caveat, we can immediately apply the results of the preceding section to the calculation of moments up to order m. Equation 22 still applies provided we use $\mathbb{L}(s)$ in place of $\mathbb{M}(s)$. So, if it is known how to write down the matrix $\mathbb{L}$ for dynamics of the chromophore, including semiclassical interactions with the radiation field, it becomes trivially easy to extract photon-counting moments. In practice, $\mathbb{L}$ may reflect either Hamiltonian chromophore dynamics with the addition of field interactions[19,20,22] or additional dissipative interactions with an environment treated implicitly as in Redfield dynamics[29,36] or some combination of Hamiltonian dynamics with stochastic modulation.[19,20,27]

From a conceptual standpoint, quantum dynamics do little to alter the generating function approach. In summary, we make the following additions to our running list of key points:

9. Application of GF techniques to quantum models requires that photon emission be handled as a rate process. Since the usual semiclassical treatments rest on this assumption, this is not a serious limitation for most chemical applications.

10. Multiple levels of quantum dynamics may be treated within the GF formalism. Pure Liouvillian dynamics, supplemented with semiclassical field interactions are possible as are treatments that involve further approximations. Removing fast and weakly coupled environmental degrees of freedom to provide a Redfield description for system dynamics is possible as are schemes involving stochastic environmental fluctuations that modulate the Liouvillian operator. What all these schemes have in common is a linear dynamics that may be written in the form of eq 26.

V. Examples

Explicit examples of stochastic dynamics were already detailed in section III, and we choose here two examples with various levels of underlying quantum dynamics to demonstrate the wide applicability of the GF formalism. Although many phenomena of interest to SMS may be treated in the context of stochastic models and indeed most of the theoretical work to date has focused on such pictures, a quantum treatment allows for studying effects of excitation frequency on photon statistics and (in some cases) emission frequency as well. In addition, quantum models for chromophore dynamics have the ability to predict behaviors based on first principles whereas purely kinetic treatments typically rely on some level of empiricism to generate the required suite of rate constants. And, of course, phenomena reliant upon quantum coherence cannot be captured within purely stochastic schemes.

An elementary and experimentally relevant example of condensed-phase chromophore dynamics is the behavior of a two-level chromophore coupled to a stochastically fluctuating two-level system (TLS). As indicated above, the TLS picture is the standard model for glassy dynamics at low temperatures, and many early single-molecule experiments probed exactly these dynamics. The standard mathematical description for a quantum mechanical two-level chromophore under laser irradiation are the optical Bloch equations[30,35]

$$\dot{\rho}_{ee} = i\Omega(\rho_{eg} - \rho_{ge})\cos(\omega_L t) - \Gamma\rho_{ee}$$

$$\dot{\rho}_{gg} = -i\Omega(\rho_{eg} - \rho_{ge})\cos(\omega_L t) + \Gamma\rho_{ee}$$

$$\dot{\rho}_{ge} = -i\omega_0(t)\rho_{ge} - i\Omega(\rho_{ee} - \rho_{gg})\cos(\omega_L t) - \frac{\Gamma}{2}\rho_{ge}$$

$$\dot{\rho}_{eg} = i\omega_0(t)\rho_{eg} + i\Omega(\rho_{ee} - \rho_{gg})\cos(\omega_L t) - \frac{\Gamma}{2}\rho_{eg} \tag{29}$$

We denote the chromophore excited and ground states as $|e\rangle$ and $|g\rangle$, respectively; $\hbar\omega_0(t)$ is a temporally evolving splitting between these two levels reflecting TLS dynamics, Ω is the Rabi frequency,[35] and ω_L is the frequency of the applied laser field; Γ is the spontaneous emission rate. The explicit time dependence within these equations is conveniently removed by invoking the rotating wave ap-

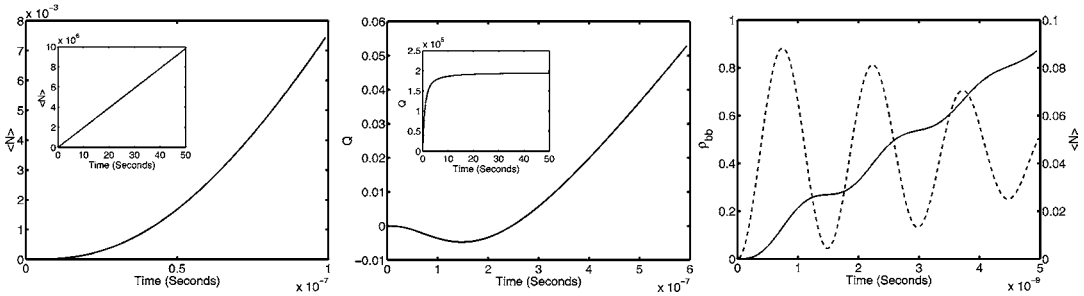

FIGURE 4. Photon statistics for a chromophore coupled to a stochastic TLS. Parameters are as described in the text except for the rightmost panel, which incorporates a Rabi frequency of 400 MHz (i.e., 100× that of the other two panels.) Inset boxes display behaviors over long time intervals. The right panel superimposes the behavior of the excited-state population (dotted line) with photon number (solid line). The effect of Rabi oscillations on the emission is apparent. Adapted from ref 19.

proximation (RWA) and introducing the "Bloch vector" notation.[35]

$$u \equiv \frac{1}{2}(\rho_{ge}\, e^{-i\omega_L t} + \rho_{eg}\, e^{i\omega_L t})$$

$$v \equiv \frac{1}{2i}(\rho_{ge}\, e^{-i\omega_L t} - \rho_{eg}\, e^{i\omega_L t})$$

$$w \equiv \frac{1}{2}(\rho_{ee} - \rho_{gg})$$

$$y \equiv \frac{1}{2}(\rho_{ee} + \rho_{gg}) \tag{30}$$

resulting in the optical Bloch equations in their conventional form

$$\dot{u} = -\frac{\Gamma}{2}u + \delta_L(t)v$$

$$\dot{v} = -\delta_L(t)u - \frac{\Gamma}{2}v - \Omega w$$

$$\dot{w} = \Omega v - \Gamma w - \frac{\Gamma}{2}$$

$$\dot{y} = 0 \tag{31}$$

where $\delta_L(t) = \omega_L - \omega_0(t)$ is the time-dependent detuning frequency. Proceeding in the manner outlined in the previous section, we obtain the generating function analogue to these equations

$$\dot{\mathcal{U}} = -\frac{\Gamma}{2}\mathcal{U} + \delta_L(t)\,\mathcal{V}$$

$$\dot{\mathcal{V}} = -\delta_L(t)\,\mathcal{U} - \frac{\Gamma}{2}\mathcal{V} - \Omega\,\mathcal{W}$$

$$\dot{\mathcal{W}} = \Omega\,\mathcal{V} - \frac{\Gamma}{2}(1+s)\,\mathcal{W} - \frac{\Gamma}{2}(1+s)\mathcal{Y}$$

$$\dot{\mathcal{Y}} = -\frac{\Gamma}{2}(1-s)\,\mathcal{W} - \frac{\Gamma}{2}(1-s)\mathcal{Y} \tag{32}$$

where, for example, $\mathcal{Y}(s,t) \equiv {}^1/_2(G_{ee}(s,t) + G_{gg}(s,t))$ and similarly for the other variables in an obvious notation paralleling eq 30. Note that our "rule" ($+\Gamma \rightarrow s\Gamma$) for formation of the GF matrix does not directly hold in the Bloch vector basis (although it does hold when dealing directly with eq 29, which is how eq 32 is derived[19,20]). This slight annoyance is far offset, by the advantages of the Bloch vector picture. In particular, the absence of field-induced explicit time dependence in $\mathbb{L}(s)$ makes for efficient numerical calculation. The TLS modulation of dynamics enters by way of $\delta_L(t)$, which is assumed to hop between two splitting energies as the TLS changes state. Internal dynamics of the TLS are assumed to follow eq 23 with both rates equal, denoted R, for simplicity. The fact that TLS dynamics are assumed to follow a Markovian dynamics allows us to remove the explicit time dependence in the detuning by extending our GF equations of motion 2-fold. The procedure is completely analogous to the purely stochastic model discussed previously and has been detailed in refs 19 and 20.

In Figure 4, we illustrate some behavior associated with this mixed quantum/stochastic model. There we choose model parameters appropriate to the spectroscopy of a dye molecule in a low-temperature glass, namely, $\Gamma = 40$ MHz, $\Omega = 4$ MHz, and $R = 1$ Hz. The laser is assumed on resonance when the system is in one of the possible TLS states ($\delta_L = 0$) and badly off resonance in the other state ($\delta_L = 2$ GHz). The initial condition reflects ground electronic state occupation at $t = 0$ and equal occupation of TLS states as dictated by thermal equilibrium. As in the purely stochastic model for chromophore/TLS dynamics, a steady-state emission rate of photons is reached following a brief relaxation to this behavior after the driving field is turned on. Similarly, Mandel's Q parameter eventually settles into a constant bunching behavior, reflecting TLS dynamics. Leading up to this behavior, antibunching is observed at short times. One behavior captured with the quantum model not observable in the classical stochastic treatment is the appearance of Rabi oscillations for sufficiently strong driving fields. These oscillations are due to coherence within the chromophore and are completely missed in the stochastic treatment.

As an example of quantum evolution, we consider the case of a chromophore with vibrational structure, modeled as a single harmonic oscillator coordinate. Details for this model are provided in ref 29, and our discussion here will be quite terse. We emphasize that although the matrix $\mathbb{L}$ for this model is more elaborate than in preceding cases, calculation of photon-counting moments proceeds in exactly the same fashion as for simpler models. Internal relaxation of the vibrational coordinate is handled through linear coupling to a harmonic bath. Effects of the bath

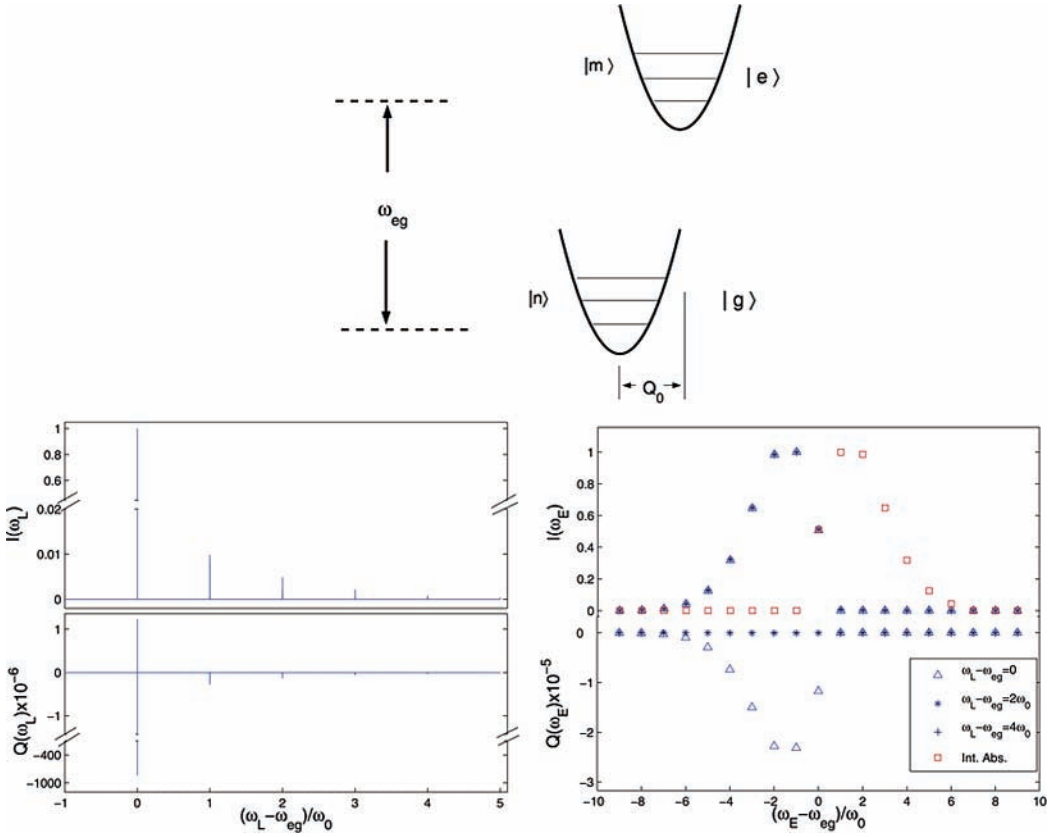

FIGURE 5. Photon statistics for a chromophore with a harmonic vibrational degree of freedom. Absorption spectrum and associated Q spectrum are seen in the left plot (calculated in the steady-state limit). Parameters were chosen such that linear response results and the exact GF calculation agree for the absorption line shapes. (The apparent positive and negative value for Q at $\omega_L - \omega_{eg} = 0$ reflects rapid variation of Q in the immediate vicinity of this point.[29]) Emission spectra are shown on the right and correspond to a variety of exciting fields. The squares represent the results from the absorption calculations integrated over the individual peaks to explicitly display the mirror symmetry between absorption and emission for this linear-response regime calculation. Adapted from ref 29.

are included implicitly in the equations of motion of the electronic, single oscillator system through application of standard Redfield theory.[36,37] As in our previous models, electronic relaxation is allowed through spontaneous emission and the excitation field is handled semiclassically. The couplings between ground and electronic manifolds are calculated within the Condon approximation for transition dipoles. In Figure 5 (left plot), we show the calculated absorption spectrum and associated Q parameter spectrum evaluated in the steady-state limit.

Physical parameters for Figure 5 were chosen to display results consistent with linear response theory for both the absorption and emission line shapes.[29] Coupling between the vibrational coordinate and the bath is tuned so that vibrational relaxation is sufficiently fast to ensure a relaxed thermal occupation of vibrational levels in both the ground and excited states when the applied field on. Additionally, the Rabi frequency of the exciting field was chosen small enough (relative to spontaneous emission rates) to ensure nearly all population resides in the ground electronic manifold at steady state. The frequency of the vibrational coordinate, ω_0, is much higher than thermal energy scales, so effectively all vibrational population resides in the vibrational ground state (regardless of the electronic state). Under these conditions, the zero phonon absorption line (0−0) is much narrower (and correspondingly taller) than the spectroscopic lines associated with transitions to higher vibrational levels (left plot of Figure 5). Transitions to higher levels are broadened by interactions with the bath, while the line width of the 0−0 line is dominated by radiative decay back to the ground state (which we chose 100 fold slower than vibrational relaxation). Integrating the absorption lines gives the result shown with squares in the right plot; these "line" heights reflect the Condon overlaps of the possible transitions out of the system's ground (electronic and vibrational) state.

While the absorption line shape can be easily predicted by linear response theory, the corresponding Q parameter calculation is not simply calculated within existing linear response frameworks and our calculation provides this information as well (see however ref 26 for an alternative methodology). Q parameter as a function of excitation frequency is recorded in the lower half of the panes of Figure 5. The parameter regime selected here ensures quite small values for the Q parameter. Other parameter regimes can lead to sizable Q values.[29]

Since this model displays vibrational structure with line widths much smaller than level spacings, it would be possible to experimentally differentiate between photons emitted in different transitions by the representative colors associated with these transitions. The right plot of Figure 5 shows calculated emission spectra inferred by counting

all transitions with different frequencies separately; that is, we assign different auxiliary variables to the spontaneous emissions occurring at the various allowed frequencies. Note the Stokes shift in the emission spectrum and the fact that we can calculate corresponding Q spectra for the spectrally resolved case. It is worth emphasizing the differences in Q spectra from the absorption and emission panes of the figure. Absorption Q calculations count all emitted photons identically and calculate statistics as a function of exciting laser frequency. Emission Q calculations consider emissions with different energy splittings between the states as different; a unique auxiliary variable is introduced for each allowed transition frequency. Laser frequency is held constant (the figure shows three different excitation frequencies), and photon statistics are collected for each emitted color separately. We do not capture the Lorentzian broadening of transitions with this technique, nor could we directly compare with experiment if individual transitions were not well resolved. Our theoretical observables are differentiated by transition, whereas experiment is sensitive only to frequency. However, we do reproduce linear response results for the emission spectrum (mirror image of the integrated absorption as expected for our parameter regime) in this case and the corresponding Q parameter spectrum. Note the quantitative difference in Q parameter values in the emission case, both relative to absorption and depending upon excitation frequency. While these numbers are easily inferred from the absorption values for this limiting parameter regime, competition among various physical time scales in general cases can lead to interesting results.[29] Monitoring higher order photon statistics yields enhanced information on system dynamics relative to line shapes alone.

VI. Conclusion

The continual evolution of experimental single-molecule techniques dictates that new theories and computational algorithms be developed for the purpose of interpreting SMS measurements. The inherently discrete nature of data in a large class of SMS experiments makes the GF approach an appealing theoretical tool for a broad range of SMS problems. We have reviewed here the application of such approaches to experiments that measure photon-counting statistics. Extension to blinking experiments and related measurements is immediate as the GF approach applies to any linear, memory-less dynamics where the counted events are pure rate processes.

The GF technique is useful as a practical numerical tool since it allows us to translate well-established methods for dynamics of the chromophore (master equations, optical Bloch equations, Redfield equations, etc.) into equations that predict the observables attainable by SMS. Although the equations will become more and more computationally expensive as higher order moments are calculated, the programming effort in extending traditional calculations is negligible. As such, the GF approach is especially appealing for testing hypothetical models against experimental data. Especially in the context of stochastic models for dynamics, it is easy to write down the hypothetical master equation which is immediately translated into GF equations of motion, suitable for simple numerical "experiments".

The research summarized herein was supported in part by the Research Corporation and the National Science Foundation. I thank Yujun Zheng and Golan Bel for their contributions to the work reviewed here.

References

(1) Moerner, W. E.; Kador, L. Optical Detection and Spectroscopy of Single Molecules in a Solid. *Phys. Rev. Lett.* **1989**, *62*, 2535−2538.
(2) Orrit, M.; Bernard, J. Single Pentacene Molecules Detected by Fluorescence Excitation in a *p*-Terphenyl Crystal. *Phys. Rev. Lett.* **1990**, *65*, 2716−2719.
(3) Gurrieri, S.; Rizzarelli, E.; Beach, D.; Bustamante, C. Imaging of Kinked Configurations of DNA Molecues Undergoing Orthogonal Field Alternating Gel Electrophoresis by Fluorescence Microscopy. *Biochemistry* **1990**, *29*, 3396−3401.
(4) Funatsu, T.; Harada, Y.; Tokunaga, M.; Saito, K.; Yanagida, T. Imaging of Single Fluorescent Molecules and Individual ATP Turnovers by Single Myosin Molecules In Aqueous-Solution. *Nature* **1995**, *374*, 555−559.
(5) Perkins, T. T.; Smith, D. E.; Larson, R. G.; Chu, S. Stretching of a Single Tethered Polymer in a Uniform Flow. *Science* **1995**, *268*, 83−87.
(6) Noji, H.; Yasuda, R.; Yoshida, M.; Kinosita, K. Direct Observation of the Rotation of F1-ATPase. *Nature* **1997**, *386*, 299−302.
(7) Plakhotnik, T.; Donley, E. A.; Wild, U. P. Single-Molecule Spectroscopy. *Annu. Rev. Phys. Chem.* **1997**, *49*, 181−212.
(8) Moerner, W. E.; Orrit, M. Illuminating Single Molecules in Condensed Matter. *Science* **1999**, *283*, 1670−1676.
(9) Xie, X. S. Single-Molecule Approach to Dispersed Kinetics and Dynamic Disorder: Probing Conformational Fluctuation and Enzymatic Dynamics. *J. Chem. Phys.* **2002**, *117*, 11024−11032.
(10) Weiss, S. Fluorescence Spectroscopy of Single Biomolecules. *Science* **1999**, *283*, 1676−1683.
(11) Bohmer, M.; Enderlein, J. Fluorescence Spectroscopy of Single Molecules under Ambient Conditions: Methodology and Technology. *ChemPhysChem* **2003**, *4*, 793−808.
(12) Lippitz, M.; Kulzer, F.; Orrit, M. Statistical Evaluation of Single Nano-Object Fluorescence. *ChemPhysChem* **2005**, *6*, 770−789.
(13) Jung, Y.; Barkai, E.; Silbey, R. J. Current Status in Single Molecule Spectroscopy: Theoretical Aspects. *J. Chem. Phys.* **2002**, *117*, 10980−10995.
(14) Feller, W. *An Introduction to Probability Theory and Its Applications*, 3rd ed.; John Wiley and Sons: New York, 1957.
(15) van Kampen, N. G. *Stochastic Processes in Physics and Chemistry*; North-Holland: Amsterdam, 1992.
(16) Gardiner, C. W. *Handbook of Stochastic Methods for Physics, Chemistry and the Natural Sciences*, 2nd ed.; Springer-Verlag: Berlin, 1985.
(17) Brown, F. L. H. Single Molecule Statistics with Time Dependent Rates: A Generating Function Approach. *Phys. Rev. Lett.* **2003**, *90*, No. 028302.
(18) Gopich, I. V.; Szabo, A. Statistics of Transitions in Single Molecule Kinetics. *J. Chem. Phys.* **2003**, *118*, 454−455.
(19) Zheng, Y.; Brown, F. L. H. Single-Molecule Photon Counting Statistics via Generalized Optical Bloch Equations. *Phys. Rev. Lett.* **2003**, *90*, No. 238305.
(20) Zheng, Y.; Brown, F. L. H. Photon Emission from Driven Single Molecules. *J. Chem. Phys.* **2003**, *119*, 11814−11828.
(21) Mukamel, S. Photon Statistics: Nonlinear Spectroscopy of Single Quantum Systems. *Phys. Rev. A* **2003**, *68*, No. 063821.
(22) Cook, R. J. Photon Number Statistics in Resonance Fluorescence. *Phys. Rev. A* **1981**, *23*, 1243−1250.
(23) He, Y.; Barkai, E. Influence of Spectral Diffusion on Single-molecule Photon Statistics. *Phys. Rev. Lett.* **2004**, *93*, No. 068302.
(24) He, Y.; Barkai, E. Super- and Sub-Poissonian Photon Statistics for Single Molecule Spectroscopy. *J. Chem. Phys.* **2005**, *122*, No. 184703.
(25) Gopich, I. V.; Szabo, A. Theory of Photon Statistics in Single-Molecule Forster Resonance Energy Transfer. *J. Chem. Phys.* **2005**, *122*, No. 014707.
(26) Sanda, F.; Mukamel, S. Liouville-Space Pathways for Spectral Diffusion in Photon Statistics from Single Molecules. *Phys. Rev. A* **2005**, *71*, No. 033807.

(27) Zheng, Y.; Brown, F. L. H. Single Molecule Photon Emission Statistics for Non-Markovian Blinking Models. *J. Chem. Phys.* **2004**, *121*, 3238−3252.
(28) Zheng, Y.; Brown, F. L. H. Single Molecule Photon Emission Statistics in the Slow Modulation Limit. *J. Chem. Phys.* **2004**, *121*, 7914−7925.
(29) Bel, G.; Zheng, Y.; Brown, F. L. H. Single Molecule Photon Counting Statistics for Quantum Mechanical Chromophore Dynamics. *J. Phys. Chem.* Submitted for publication, 2006.
(30) Loudon, R. *The Quantum Theory of Light*, 3rd ed.; Oxford: New York, 2000.
(31) Mandel, L. Sub-Poissonian Photon Statistics in Resonance Fluorescence. *Opt. Lett.* **1979**, *4*, 205−207.
(32) Michler, P.; Imamoglu, A.; Mason, M. D.; Carson, P. J.; Strouse, G. F.; Buratto, S. K. Quantum Correlation among Photons from a Single Quantum Dot at Room Temperature. *Nature* **2000**, *406*, 968−970.
(33) Anderson, P. W.; Halperin, B. I.; Varma, C. M. Anomalous Low-Temperature Thermal Properties of Glasses and Spin Glasses. *Philos. Mag.* **1972**, *25*, 1−9.
(34) Zwanzig, R. Rate Processes with Dynamical Disorder. *Acc. Chem. Res.* **1990**, *23*, 148−152.
(35) Cohen-Tannoudji, C.; Dupont-Roc, J.; Grynberg, G. *Atom-Photon Interactions*; Wiley-Interscience: New York, 1992.
(36) Blum, K. *Density Matrix Theory and Applications*, 2nd ed.; Plenum Press: New York, 1981.
(37) Schatz, G.; Ratner, M. *Quantum Mechanics in Chemistry*; Prentice Hall: Englewood Cliffs, NJ, 1993.

AR050028L